

## XANES INVESTIGATION OF MOLYBDATE CATALYSTS SUPPORTED ON TITANIA

Lukas M. J. von HIPPEL<sup>a</sup>, Frank HILBRIG<sup>a,b</sup>, Helmut SCHMELZ<sup>b,\*</sup>,  
Bruno LENGELER<sup>c</sup> and Helmut KNÖZINGER<sup>a,\*\*</sup>

<sup>a</sup>*Institut für physikalische Chemie,  
Universität München, Sophienstr. 11, 8000 Munich-2, Germany*

<sup>b</sup>*Siemens AG, Bereich Energieerzeugung,  
Otto-Hahn-Ring 6, 8000 Munich-83, Germany*

<sup>c</sup>*Institut für Schicht- und Ionentechnik der KFA Jülich,  
Postfach 1913, 5770 Jülich-1, Germany*

Received June 2, 1992  
Accepted June 20, 1992

*Dedicated to Dr Miloš Kraus on the occasion of his 65th birthday.*

---

Molybdenum oxide supported on titania is an important material for catalytic processes in petroleum industry as well as in air pollution control. A structure analysis by means of X-ray absorption spectroscopy (XANES) is reported for samples prepared by spreading of MoO<sub>3</sub> in physical mixtures with the support as well as by impregnation from aqueous solution. Analysis of the XANES region of the Mo K edge indicated that the surface molybdate has a structure similar to ammonium heptamolybdate.

---

Titania-supported molybdenum-containing catalysts are active for hydrodesulfurization and hydrocracking<sup>1</sup> as well as for the metathesis of olefins<sup>2</sup> and they are industrially used for selective catalytic reduction of NO<sub>x</sub> by ammonia (SCR) in tail gases from power plants<sup>3,4</sup>. The surface structures affect the catalytic activity and selectivity. Typically this class of catalytic materials is prepared by impregnation of the support with aqueous solutions of ammonium heptamolybdate (NH<sub>4</sub>)<sub>6</sub>Mo<sub>7</sub>O<sub>24</sub> · 4 H<sub>2</sub>O. For industrial scale catalyst preparation, waste water disposal becomes more and more a serious problem. Therefore, it is necessary to develop other routes of catalyst preparation so as to reduce the amounts of waste water.

We have reported recently<sup>5-10</sup> that dispersed supported oxide catalysts (including alumina and titania supports) can be obtained from physical mixtures of the binary

---

\* Present address: Siemens KPW PK 23, Postfach 60, 8627 Redwitz.

\*\*The author to whom correspondence should be addressed.

oxides.  $\text{MoO}_3$  spreads on the surface of alumina and titania supports. Laser Raman spectra<sup>5,6,8</sup> suggested that a surface polymolybdate was formed during spreading in a humid oxygen atmosphere. In contrast, calcination in dry oxygen led to dispersed surface structures similar – if not identical – to  $\text{MoO}_3$ . Raman microscopy had demonstrated<sup>9</sup> that the transport of  $\text{MoO}_3$  on  $\text{Al}_2\text{O}_3$  surfaces occurs over macroscopic distances, i. e., several hundred micrometers under the applied experimental conditions. Solid–solid wetting is considered to be responsible for the spreading process. It is also known that the activity of these catalysts for the SCR-process increases with the addition of small amounts of vanadium oxide by a synergistic effect<sup>11,30</sup>. Therefore, it seemed to be of interest to characterize structurally several molybdate catalysts supported on titania with and without vanadium oxide which were prepared by different procedures and which contained varying amounts of molybdenum oxide.

X-ray absorption spectroscopy (XAS)<sup>12,13</sup> is a local probe of the symmetry and coordination around a given site and also provides the valence state of the absorbing central atom. EXAFS has been used to understand the structure of the molybdate species on alumina<sup>14,15</sup> and on silica<sup>12</sup>. Unfortunately, real catalysts are often not sufficiently well ordered so that EXAFS analyses may not be straightforward. In this case, XANES can provide useful information on the structure of the surface species when the corresponding spectra are compared with fingerprint spectra of suitable reference compounds. XAS has – in contrast to many other methods – the advantage that the experiments can be done in situ.

## EXPERIMENTAL

$\text{TiO}_2$  P 25 was from Degussa and had a  $\text{N}_2$  BET surface area of  $50 \text{ m}^2/\text{g}$ . It is prepared by flame hydrolysis of  $\text{TiCl}_4$  and contains 70% anatase and 30% rutile.  $\text{TiO}_2$  DT 51 was from Rhone Poulenc. It is prepared from  $\text{TiOSO}_4$  by hydrolysis and has a  $\text{N}_2$  BET surface of  $90 \text{ m}^2/\text{g}$ . This material contains at least 98% anatase.

*Physical mixtures* of 1.2 and 4.1 wt.%  $\text{MoO}_3/\text{TiO}_2$  P 25 were ground in an agate mortar and calcined at 723 K for 30 h in a moist oxygen stream (50 ml/min;  $p(\text{H}_2\text{O}) = 18 \cdot 10^2 \text{ Pa}$ ). In the following, these samples will be denoted TiMo1.2A and TiMo4.1A.

*The wet impregnated samples* with an amount of  $\text{MoO}_3$  corresponding to the theoretical monolayer capacity (6.8 wt.%) were prepared by suspending 80 g of  $\text{TiO}_2$  DT 51 in water at 343 K. An aqueous solution containing the appropriate amount of the ammonium salt  $(\text{NH}_4)_6\text{Mo}_7\text{O}_{24} \cdot 4 \text{ H}_2\text{O}$  at 343 K was added to the suspension. The resulting mixture was stirred for half an hour and the water was then removed under vacuum. The resulting material was dried overnight at 373 K in air. After crushing and sieving (particle size below 0.2 mm), the powder was calcined at 773 K for 8 h in air. This material will be denoted MonoMo in the following. For preparation of the vanadium oxide containing catalyst, the aqueous solution also contained the appropriate amount of  $\text{NH}_4\text{VO}_3$  so as to give a monolayer catalyst with a Mo : V atomic ratio of 18 : 1, all other preparation steps remaining unchanged. This material will be denoted 18Mo1V. The uncalcined materials are denoted MonoMoNC and 18Mo1VNC throughout this paper.

*The reference compounds* used for XANES analysis were Mo,  $\text{MoO}_2$ ,  $\text{MoO}_3$  (Merck),  $(\text{NH}_4)_6\text{Mo}_7\text{O}_{24} \cdot 4 \text{ H}_2\text{O}$  (Fluka),  $\text{PbMoO}_4$ ,  $\text{CaMoO}_4$ ,  $\text{SrMoO}_4$ ,  $\text{Na}_2\text{MoO}_4$  and  $\text{Ba}_3\text{TiMoO}_8$ .  $\text{Ba}_3\text{TiMoO}_8$  was prepared by tempering a 3 : 1 : 1 mixture of  $\text{BaCO}_3$ ,  $\text{MoO}_3$  and  $\text{TiO}_2$  in a Pt-crucible at 1 473 K for 24 h. The purity

detected by XRD was better than 98%.  $\text{Na}_2\text{MoO}_4$  was prepared from  $\text{Na}_2\text{MoO}_4 \cdot 2 \text{H}_2\text{O}$  (Merck) by dehydration at 400 K.

*The X-ray absorption experiments* at the Mo K edge were carried out at the beam line E 2 of the electron storage ring DORIS II (3.7 GeV, 40 – 100 mA) at the Hamburg Synchrotron Laboratories HASY-LAB at the Deutsches Elektronen Synchrotron DESY. The experimental setup was described elsewhere<sup>17</sup>. An Si (311) doublecrystal monochromator was used which had an energy resolution better than 6 eV at the Mo K edge<sup>18</sup>. The harmonic content was reduced below 1 part in  $10^4$  by detuning the monochromator crystals. The experiments were carried out in the transmission mode using ionisation chambers containing  $\text{N}_2$  in the first chamber (approx. 10% absorption) and a mixture of  $\text{N}_2$  and Ar in the second (approx. 95% absorption). The energy calibration was performed by measuring a Mo-foil simultaneously with the sample using a third ionization chamber in series.

*The high-temperature experiments* were carried out in an in situ cell<sup>19</sup> at 673 K in air atmosphere enriched with oxygen. For the high-temperature experiments, the sample powders (TiMo1.2 and TiMo4.1) were slightly pressed into an aluminium frame (0.5 mm thick) over an area of  $10 \times 25 \text{ mm}^2$  and enveloped in aluminium foil. The XAS-experiments at room-temperature (MonoMo, MonoMoNC, 18Mo1V and 18Mo1V and 18Mo1VNC) were carried out using an aluminium cuvette with windows made from aluminium foil allowing a sample thickness of 2 mm. For the reference compounds, the finely ground powder was spread out on a Kapton adhesive tape so as to achieve an optimal sample thickness. The reference samples have been measured at 77 K. The linear absorption coefficient multiplied by the sample thickness  $\mu(E)d$  was determined in the vicinity of the edge energy. The XANES spectra were normalized by fitting a linear function to the pre-edge data and to the EXAFS-region, extrapolating both functions to the zero of energy  $E_0$ , subtracting the background from each point in the experimental spectrum and deviding by the step height at  $E_0$ .  $E_0$  is defined as the point of inflection of the Mo K absorption edge. This procedure results in a normalization of the data to unit step height and eliminates the sample thickness. The EXAFS have not been calculated since the samples showed only a first coordination shell. A second coordination shell could not be observed because of poorly ordered surface species.

## RESULTS AND DISCUSSION

All samples were analysed by X-ray diffraction (XRD) and Raman spectroscopy. No crystalline structures of molybdenum and vanadium oxides could be detected by XRD in any of the calcined samples. Only the expected diffraction patterns of anatase (and rutile) were obtained. The Raman spectra of all samples showed the characteristic broad feature near  $950 \text{ cm}^{-1}$  of Mo=O stretching modes indicating the presence of surface structures in all samples<sup>5-9</sup>. The characteristic sharp lines of  $\text{MoO}_3$  were not observed in anyone of the samples. These results are consistent with the formation of highly dispersed surface molybdate structures in all samples, although the detailed molecular surface structures cannot be deduced, so that XAS is expected to provide the necessary additional information.

The fine structure of an X-ray absorption edge is directly related to the local density of final states<sup>20</sup>. Band structure calculations based on a known geometric structure allow calculations of the linear absorption coefficient. Without band structure calculation, the position and the fine structure of an absorption edge can be used as a "fingerprint" for changes in the valence and in the local arrangement of the neighboring

atoms around the absorber atom<sup>21-23</sup> in comparison with reference compounds, which can have different crystallographic structures.

Depending on the local geometry, electronic excitations are observed. In the most simple interpretation, a pseudo-atomic model leads to the result, that the observed structures may be due to  $1s \rightarrow 4d$ ,  $1s \rightarrow 5s$  and  $1s \rightarrow 5p$  transitions<sup>24</sup>. In a tetrahedral oxygen sphere the first of these transitions is partially allowed because of  $d$ - $p$  orbital mixing, but it is strictly forbidden in an octahedral field. This selection rule is no longer valid when the octahedral symmetry is perturbed. Chiu et al.<sup>24</sup> defined the so-called *NUD* number

$$NUD = \frac{1}{p} \sum_{i=1}^p \frac{R_i - R_m}{R_m} \quad (1)$$

where  $R_m$  is the arithmetic mean of the Mo-O distances and  $R_i$  an individual Mo-O distance. The *NUD* number is a measure of the extent of distortion of the octahedral symmetry of oxygen atoms in the first oxygen coordination shell. The *NUD* number could not explain all experimentally observed details. Therefore, Chiu et al.<sup>24</sup> also included a correction, called *NUA* number, for the distortion of the angles between the Mo-O bonds (i. e. the direction of the hybrid orbitals). However, the *NUD* and *NUA* numbers for the investigated Mo-catalysts could not be calculated. Wong et al.<sup>25</sup> could show that for vanadium oxides the "molecular cage effect" is responsible for the intensity of the  $s \rightarrow d$  transition. The "molecular cage effect" relates to the average V-O distances in the first coordination sphere. The reduction of the coordination number increases the oscillator strength. The oscillator strength decreases, if the average bond length increases in the same class of polyhedra. This shows the importance of reference compounds with structure resemblance as close as possible to the unknown structure. It also shows that not only the pre-edge region of a XANES-spectrum helps to understand the investigated species. A comparison of the structures beyond the absorption edge may also help to distinguish between different structures.

Figure 1 displays the Mo K edge of the reference compounds Mo, MoO<sub>2</sub> and MoO<sub>3</sub>. It is obvious, that the edge position shifts with higher oxidation state to higher energy as expected. MoO<sub>2</sub> shows no pre-edge peak. The rutile structure of MoO<sub>2</sub> consists of distorted octahedra<sup>26</sup>, but the *NUD* number 0.018 is very low. MoO<sub>3</sub> has four short Mo-O distances between 1.67 Å and 1.94 Å which form a structure close to a tetrahedron, and two long distances of 2.25 Å and 2.33 Å which complete the distorted octahedral coordination<sup>27</sup>. As a consequence, a *NUD* number greater than that of MoO<sub>2</sub>, namely 0.105 (ref.<sup>24</sup>) results and a prominent pre-edge peak develops.

In Fig. 2, the Mo K edges of Ba<sub>3</sub>TiMoO<sub>8</sub>, Na<sub>2</sub>MoO<sub>4</sub> and MoO<sub>3</sub> are compared. Na<sub>2</sub>MoO<sub>4</sub> is composed of nearly ideal MoO<sub>4</sub> tetrahedra with a Mo-O distance of 1.76 Å. Ba<sub>3</sub>TiMoO<sub>8</sub> consists of TiO<sub>4</sub> and MoO<sub>4</sub> tetrahedra. Both compounds give rise to a characteristic pre-edge peak at lower energy as compared to distorted octahedral structures.

The different long-range order is manifested in the XANES structure at the high energy side relative to the absorption edge. The spectrum of  $\text{MoO}_3$  was discussed above.

Figure 3 shows the Mo K edges of  $\text{Na}_2\text{MoO}_4$ ,  $\text{CaMoO}_4$ ,  $\text{SrMoO}_4$  and  $\text{PbMoO}_4$ . In all these compounds, Mo is tetrahedrally surrounded by oxygen.  $\text{PbMoO}_4$  for example has Mo–O distances of 1.77 Å and only the angles between the Mo–O bond vary<sup>27</sup> between 113° and 105°. All these oxides crystallize in the Scheelite structure. The lattice parameters of these various molybdates and the angles between Mo–O bonds vary. This leads to spectra showing a sharp pre-edge peak with nearly the same position and magnitude in all cases but the XANES structures become less pronounced with increasing atomic weight of the cation. A deviation from ideal tetrahedral environment leads to significant differences in the XANES region. A similar behaviour is also observed for octahedral coordination: Fig. 4 compares the spectra of  $\text{MoO}_3$  and ammonium heptamolybdate  $(\text{NH}_4)_6\text{Mo}_7\text{O}_{24} \cdot 4 \text{H}_2\text{O}$ . Both compounds having distorted octahedral symmetry around Mo show a pre-edge peak with nearly the same position and intensity, their respective XANES regions up to 30 eV beyond the Mo K edge, however, showing significant differences. These can be related with the different structures of  $\text{MoO}_3$  and  $(\text{NH}_4)_6\text{Mo}_7\text{O}_{24} \cdot 4 \text{H}_2\text{O}$  and will help to distinguish between different molybdenum oxides.

The Mo K edge spectra of the uncalcined and calcined impregnated samples are shown in Fig. 5. It is obvious that the spectra of corresponding uncalcined and calcined samples are identical and very closely resemble that of the heptamolybdate shown in Fig. 4b. This suggests that the heptamolybdate anion adsorbs intact from solution and that the following calcination does not affect the local geometry. This stabilization of

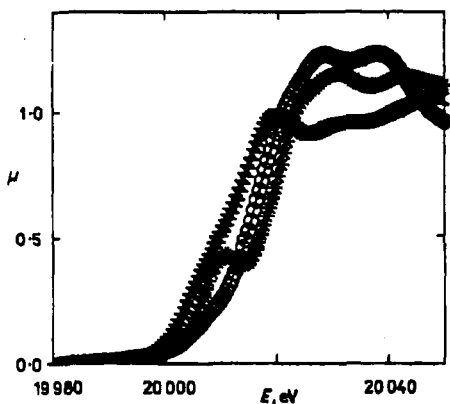


FIG. 1  
Mo K edges of Mo (x),  $\text{MoO}_2$  (O) and  $\text{MoO}_3$  (\*)

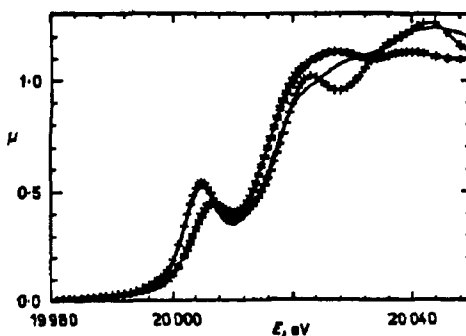


FIG. 2  
Mo K edges of  $\text{Ba}_3\text{TiMoO}_8$  (—),  $\text{Na}_2\text{MoO}_4$  (+) and  $\text{MoO}_3$  (\*)

the heptamolybdate anion on calcination has also been found on  $\text{Al}_2\text{O}_3$ -supports<sup>28,29</sup>. The addition of small amounts of vanadium oxide has no measurable effect on the Mo K edge structure neither before nor after the calcination (Figs 5c and 5d). Two reasons may be responsible for this behaviour. It is possible that the vanadium is not in contact with the molybdates and can therefore not influence the local structure. This would be in contrast to the observed synergistic increase of the activity and selectivity for the SCR process when vanadium oxide is present<sup>11,30</sup>. The second, more likely reason may be that the presence of vanadium oxide leads to a surface structure similar to the heptamolybdate. It is known<sup>31</sup> that small amounts of vanadium oxide can be incorporated in a heteropolymolybdate structure. In this case, XANES can not distinguish between the different molybdates.

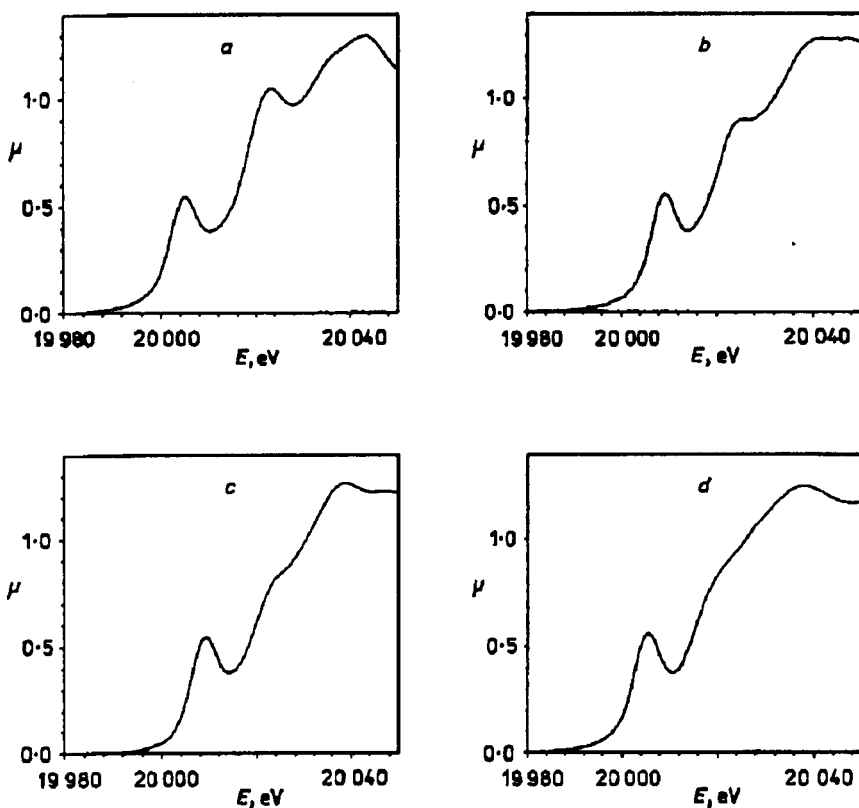


FIG. 3  
Mo K edges of  $\text{Na}_2\text{MoO}_4$  (a),  $\text{CaMoO}_4$  (b),  $\text{SrMoO}_4$  (c) and  $\text{PbMoO}_4$  (d)

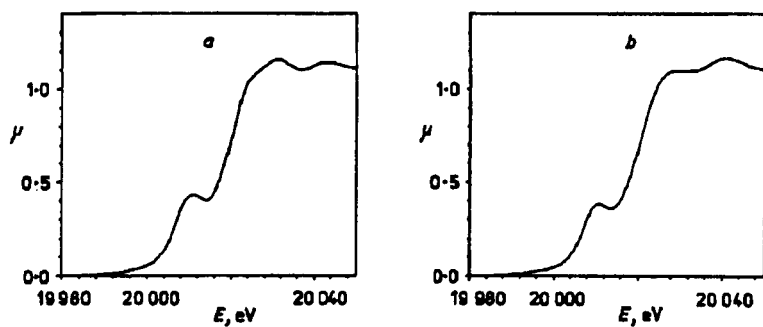


FIG. 4  
Mo K edges of  $\text{MoO}_3$  (a) and  $(\text{NH}_4)_6\text{Mo}_7\text{O}_{24} \cdot 4 \text{H}_2\text{O}$  (b)

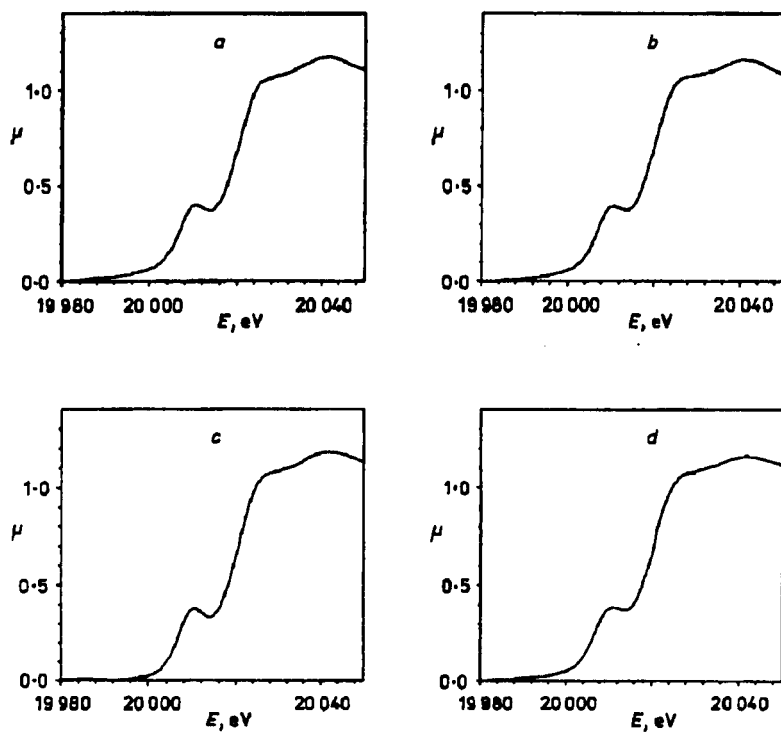


FIG. 5  
Mo K edges of MonoMoNC (a), MonoMo (b), 18Mo1VNC (c) and 18Mo1V (d)

Figure 6 shows the Mo K edges of the catalysts TiMo4.1A and TiMo1.2A prepared from physical mixtures of MoO<sub>3</sub> and TiO<sub>2</sub> P 25. The spectra of both samples contain a prominent pre-edge peak with, however, different intensities and positions: The signal from TiMo1.2A appears at lower energy and is more intense than the peak from TiMo4.1A. In contrast to the other experiments, these samples have been measured at 673 K and were thus dehydrated. The monolayer capacity for TiO<sub>2</sub> P 25 is reached at 4.1 wt.% when MoOCl<sub>4</sub> is grafted onto the TiO<sub>2</sub> P 25 surface<sup>32</sup>. Therefore, TiMo4.1A contains a MoO<sub>3</sub> amount corresponding to a theoretical monolayer, while TiMo1.2A contains only 30% of the monolayer capacity. In direct comparison with the references, both samples show a higher similarity with ammonium heptamolybdate in the XANES region of the edge and at higher energies than with other reference samples. It is thus inferred that a calcination of a physical mixture of MoO<sub>3</sub> and TiO<sub>2</sub> in moist oxygen leads to a similar structure of the surface molybdate as after the impregnation with an aqueous solution of the ammonium heptamolybdate.

This inference is also consistent with the position and intensity of the pre-edge peak observed for TiMo4.1A containing a monolayer of molybdenum oxide. Hence, the experimental evidence here is in favour of the formation of a surface molybdate structure with Mo in distorted octahedral symmetry as already indicated by the Raman spectra of this material. For the sample TiMo1.2A containing only 30% of a monolayer of molybdenum oxide, the pre-edge peak is slightly more intense and shifted toward lower energy. These trends point toward possible contributions of Mo species having lower oxygen-coordination number, e.g. in tetrahedral symmetry. It is likely that at lower loadings tetrahedral, perhaps monomeric, and possibly pentacoordinated Mo species particularly in the dehydrated state of the catalyst do exist on the catalyst surface as under the present experimental conditions. Analogous trends have recently been observed<sup>33</sup> with XANES and FT-IR for tungsten oxide supported on titania. It is inferred that surface structures similar to those postulated for the tungsten oxide/titania

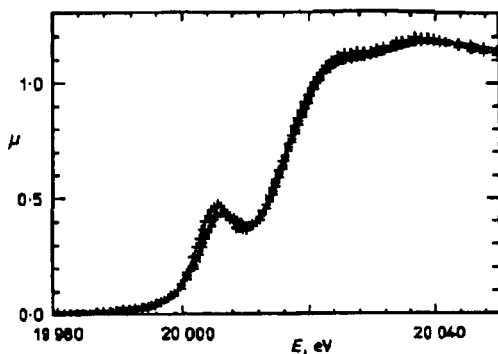


FIG. 6  
Mo K edges of TiMo1.2A (+) and  
TiMo4.1 (\*)



system would well explain the experimental results obtained at high temperature for the present  $\text{MoO}_3/\text{TiO}_2$  catalysts.

## CONCLUSIONS

The present XANES investigations indicate that the  $\text{TiO}_2$  catalysts prepared by the wet impregnation method and by the spreading method in moist oxygen contains at least similar molybdates with a structure close to ammonium heptamolybdate. This conclusion is fully consistent with the results of earlier Raman studies<sup>7,8,10</sup>. The addition of small amounts of vanadium oxide do not give rise to observable changes in the structure of the molybdate. The impregnated samples do not show any structural changes after the calcination this being indicative for the fact that the final structure is already preformed after the impregnation. At a loading below 1/3 of a monolayer smaller molybdate ensembles predominate. Different titania supports (P 25, DT 51) do not seem to affect the structure of the supported molybdate when the loading corresponds to the monolayer capacity.

*This work was financially supported by the Deutsche Forschungsgemeinschaft, the Fonds der chemischen Industrie and the Bundesministerium für Forschung und Technologie. We thank the Hasylab (DESY, Hamburg) for experimental assistance. We acknowledge the assistance of Dr H. E. Göbel, Siemens Corp., Munich, with the XRD measurements and of G. Mestl, Munich University, with the laser Raman spectroscopy.*

## REFERENCES

1. Quincy R. B., Houalla M., Proctor A., Hercules M. D.: *J. Phys. Chem.* **93**, 5882 (1989).
2. Tanaka K., Miyahara K., Tanaka K.: *Bull. Chem. Soc. Jpn.* **54**, 3106 (1981).
3. Morikawa S., Takahashi K., Yoshida H., Kurita S.: *Proc. 8th Int. Congr. Catal., Berlin 1984*, Vol. III, p. 661. Verlag Chemie, Weinheim and Dechema, Frankfurt 1984.
4. Vogt E., van Dillen J., Geus J., Bierman J., Janssen F.: *Proc. 9th Int. Congr. Catal., Calgary 1988* (M. J. Philips and M. Ternan, Eds), Vol. 5, p. 1976. The Chemical Institute of Canada, Ottawa 1988.
5. Leyrer J., Zaki M. I., Knözinger H.: *J. Phys. Chem.* **90**, 4775 (1986).
6. Margraf R., Leyrer J., Knözinger H., Taglauer E.: *Surf. Sci.* **189/190**, 842 (1987).
7. Margraf R., Leyrer J., Taglauer E., Knözinger H.: *React. Kinet. Catal. Lett.* **35**, 261 (1987).
8. Leyrer J., Margraf R., Taglauer E., Knözinger H.: *Surf. Sci.* **201**, 603 (1988).
9. Leyrer J., Mey D., Knözinger H.: *J. Catal.* **124**, 349 (1990).
10. Knözinger H., Taglauer E. in: *Catalysis* (J. J. Spivey, Ed.), Vol. 10. The Royal Society of Chemistry, Cambridge, to be published 1993.
11. Satsuma A., Hattori A., Mizutami K., Furita A., Miyamoto A., Hattori T., Murakami Y.: *J. Phys. Chem.* **93**, 1484 (1989).
12. Konigsberger D. C., Prins R. (Eds): *X-Ray Absorption: Principles and Techniques of EXAFS, SEXAFS and XANES*. Wiley, New York 1989.
13. Lengeler B.: *Festkörperprobleme* **29**, 53 (1989).
14. Clausen B. S., Lengeler B., Topsøe H.: *Polyhedron* **5**, 199 (1986).
15. Kisfaludi G., Leyrer J., Knözinger H., Prins R.: *J. Catal.* **130**, 192 (1991).

16. Caillet P.: *Bull. Soc. Chim. Fr.* 1967, 4750.
17. Lengeler B.: *Mikrochim. Acta* 1, 455 (1987).
18. Scheuer U., Lengeler B.: *Phys. Rev.*, B 44, 9883 (1991).
19. Hilbrig F.: *Thesis*. Munich University, Munich 1989.
20. Lengeler B.: *X-Ray Absorption and Reflection in the Hard X-Ray Range*, in: *Summer School "Enrico Fermi", Varenna 1988, Italy* (R. Rosei et al. Eds). North Holland, Amsterdam 1990.
21. Lengeler B.: *Z. Phys.*, B 81, 421 (1985).
22. Lengeler B.: *Adv. Mater.* 2, 123 (1990).
23. Lengeler B.: *Phys. Bl.* 86, 50 (1990).
24. Chiu N. S., Bauer S. H., Johnson M. F. L.: *J. Catal.* 89, 226 (1984).
25. Wong J., Lytle F. W., Messmer R. P., Maylotte D. H.: *Phys. Rev.*, B 30, 5596 (1984).
26. Brandt B. G., Skapski A. C.: *Acta Chim. Scand.* 21, 661 (1967).
27. Gmelin: *Handbuch der Anorganischen Chemie*, 8. Aufl., *Molybdän, Ergänzungsband B 2*. Springer Verlag, Berlin, Heidelberg, New York 1986.
28. Knözinger H.: *Proc. 9th Int. Congr. Catal., Calgary 1988* (M. J. Phillips and M. Ternan, Eds), Vol. 5, p. 20. The Chemical Institute of Canada, Ottawa 1989.
29. Butz T., Vogdt C., Lerf A. Knözinger H.: *J. Catal.* 116, 31 (1989).
30. von Hippel L. M. J., Knözinger H.: Unpublished results.
31. Kihlborg L.: *Acta Chim. Scand.* 23, 1834 (1969).
32. Bond G. C., Flamerz S., van Wijk L.: *Catal. Today* 1, 229 (1987).
33. Hilbrig F., Göbel H. E., Knözinger H., Schmelz H., Lengeler B.: *J. Phys. Chem.* 95, 6973 (1991).